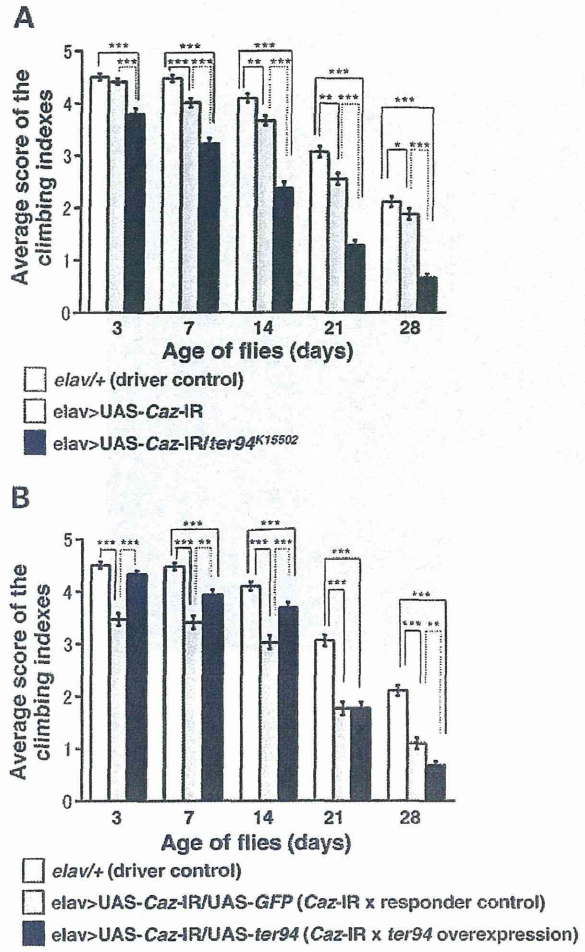

Figure 4. A loss-of-function *ter94* mutation and wild-type *ter94* overexpression have opposite effects on the climbing ability of neuron-specific *Caz*-knockdown flies. (**A**) The locomotive ability of driver control flies, which carrying *elav/+* ($n = 366$, white columns), is significantly better than that of neuron-specific *Caz*-knockdown flies, which carrying elav>UAS-*Caz*-IR ($n = 296$, gray columns) for every age examined other than day 3. On each day after eclosion that was monitored, adult flies carrying elav>UAS-*Caz*-IR/*ter94*^{K15502} ($n = 210$, black columns) exhibited significantly worse climbing ability than flies carrying neuron-specific *Caz*-knockdown alone. (**B**) Conversely, adult flies carrying elav>UAS-*Caz*-IR/UAS-*ter94* ($n = 215$, black columns) have significantly better climbing ability than flies carrying elav>UAS-*Caz*-IR/UAS-*GFP* ($n = 190$, gray columns) on days 3, 7 and 14, but not after day 14. The climbing ability of flies carrying *elav/+* ($n = 366$, white columns) is significantly better than those carrying elav>UAS-*Caz*-IR/UAS-*GFP* for every age examined, same as those in (A). Until day 3, the climbing ability of flies carrying elav>UAS-*Caz*-IR/UAS-*ter94* is recovered almost as well as that of flies carrying *elav/+*. However, that of the flies carrying elav>UAS-*Caz*-IR/UAS-*ter94* is significantly less than that of flies carrying *elav/+* after day 3. Columns and horizontal bars show the mean and SE of the measurements, respectively. $^{***}P < 0.001$, $^{**}P < 0.01$ and $^{*}P < 0.05$.

terminals at NMJs in *Caz*-knockdown flies. Abnormal NMJ morphology and behavioral defects have been implicated in many *Drosophila* models of neurodegenerative diseases that involve motor disturbances such as spinal muscular atrophy and tauopathies (30,31). Because most MNs of the adult fly originate from larval MNs, we examined the NMJ structure in the larvae from *Caz*-knockdown strains. Previously, we demonstrated that neuron-specific *Caz*-knockdown shortened terminal branches of larval MNs (19). To clarify the effects of the *ter94* mutation on the morphology of MN terminals, we examined the NMJ structure of our *Caz*-knockdown flies with or without *ter94* mutation and with or without wild-type *ter94* overexpression.

Compared with the total length of synaptic branches of MNs in driver control larvae carrying *elav/+* (94.4 ± 8.0 μm, Fig. 5A), which was significantly decreased in neuron-specific *Caz*-knockdown larvae carrying elav>UAS-*Caz*-IR (53.8 ± 6.0 μm, Fig. 5B; $P < 0.001$, Fig. 5D). Furthermore, this decreased branch length caused by neuron-specific *Caz*-knockdown was significantly enhanced by genetic crossing with the strongest loss-of-function allele of *ter94* (elav>UAS-*Caz*-IR/*ter94*^{K15502}, 39.5 ± 1.7 μm, Fig. 5C; $P = 0.035$, Fig. 5D). The average number of synaptic boutons per MN was also significantly smaller in neuron-specific *Caz*-knockdown larvae (9.7 ± 0.5, Fig. 5B) than in control larvae (14.7 ± 1.0, Fig. 5A; $P < 0.001$, Fig. 5E). This decrease in the number of synaptic boutons in the neuron-specific *Caz*-knockdown larvae was significantly enhanced by genetic crossing with the strongest loss-of-function allele of *ter94* (6.5 ± 0.5, Fig. 5C; $P < 0.001$, Fig. 5E). However, there were no significant differences in the size of synaptic boutons among these genotypes (Fig. 5F).

Conversely, the total branch length was significantly longer in the larvae with *ter94* overexpression in the background of neuron-specific *Caz*-knockdown (elav>UAS-*Caz*-IR/UAS-*ter94*, Fig. 5H and I) than in responder control larvae (elav>UAS-*Caz*-IR/UAS-*GFP*, Fig. 5G; 110.7 ± 12.0 versus 54.7 ± 2.5 μm, $P < 0.001$, Fig. 5J). The total branch length in the larvae carrying elav>UAS-*Caz*-IR/UAS-*GFP* was also significantly decreased compared with those carrying *elav/+* (94.4 ± 8.0 versus 54.7 ± 2.5 μm, $P < 0.001$, Fig. 5J). However, there were no significant differences about the total branch length between the larvae carrying *elav/+* and elav>UAS-*Caz*-IR/UAS-*ter94* (Fig. 5J). These results indicated that a loss-of-function *ter94* mutation and wild-type *ter94* overexpression have opposite effects on the synaptic terminal growth and morphogenesis that is impaired by *Caz*-knockdown. Notably, in the larvae with *ter94* overexpression in the background of neuron-specific *Caz*-knockdown (elav>UAS-*Caz*-IR/UAS-*ter94*), the extent of increase in the total branch length showed considerable variability (Fig. 5H and I). Of the larvae with *ter94* overexpression in the background of neuron-specific *Caz*-knockdown, 28% had branch lengths (Fig. 5I) that were 2-fold or more elongated relative to the responder controls (Fig. 5G). The larvae carrying elav>UAS-*Caz*-IR/UAS-*ter94* (Fig. 5H and I) also showed significantly increased number of synaptic boutons of MN terminals (25.6 ± 3.5) compared with those carrying elav>UAS-*Caz*-IR/UAS-*GFP* (8.7 ± 0.5, Fig. 5G; $P < 0.001$, Fig. 5K). The number of synaptic boutons in the larvae carrying elav>UAS-*Caz*-IR/UAS-*GFP* was also significantly decreased compared with that of those carrying *elav/+* (8.7 ± 0.5 versus 14.7 ± 1.0, $P < 0.01$, Fig. 5K). The number of synaptic boutons in the larvae carrying elav>UAS-*Caz*-IR/UAS-*ter94* was significantly increased compared with that of those carrying *elav/+* (14.7 ± 1.0 versus 25.6 ± 3.5, $P < 0.05$, Fig. 5K). The number of synaptic boutons of MNs might be increased in

the larvae carrying elav>UAS-*Caz*-IR/UAS-*ter94* due to the growth of synaptic terminals. There were no significant differences in the size of synaptic boutons among these genotypes (Fig. 5L). These results indicated that Caz is required for growth of MN terminals and formation of synaptic boutons at the NMJ, and these functions of Caz at the MN terminals are affected by the levels of ter94 protein.

DISCUSSION

Here, we demonstrated that eye-specific and neuron-specific *Caz*-knockdown induced a rough-eye phenotype and locomotive dysfunction, respectively; moreover, the locomotive dysfunction was due to the degeneration of MNs. The strongest loss-of-function allele of *ter94* (*ter94*^{k15502}) enhanced such rough-eye and locomotive-dysfunction phenotypes induced by *Caz*-knockdown. Conversely, the overexpression of wild-type *ter94* significantly suppressed the phenotypes induced by *Caz*-knockdown such as rough-eye phenotype, locomotive disabilities and degeneration of MNs. Moreover, neuron-specific *Caz*-knockdown decreased Caz levels in nuclei, and overexpression of wild-type *ter94* significantly suppressed the effects on nuclear *Caz*-expression levels induced by *Caz*-knockdown.

VCP is a member of the AAA protein family; these proteins are involved in diverse cellular functions and in a variety of physiological processes such as cell cycle regulation, membrane fusion, ER-associated degradation, ubiquitin-mediated protein degradation and nucleocytoplasmic shuttling (22–24). VCP is implicated in various neurodegenerative disorders. Mutations in the human *VCP* gene have been reported to cause frontotemporal dementia associated with IBMPFD or familial ALS, and VCP is consequently now considered as a causative gene for FTLD/ALS (25,26). Additionally, previous studies demonstrated that VCP is a binding partner of polyglutamine (polyQ) disease proteins with expanded polyQ tracts (huntingtin, ataxin-1, ataxin-3, ataxin-7 and androgen receptor) (32,33). Previously, the *Drosophila* ortholog of *VCP*, *ter94*, was identified in a screen for genetic modifiers of the eye degeneration phenotypes induced by eye-specific expression of an expanded polyQ tract (34). Moreover, VCP may be involved in diseases that are caused by changes in protein conformation; notably, VCP has been shown to colocalize with pathological protein aggregates in cases of Parkinson's disease, dementia with Lewy bodies, superoxide dismutase 1-associated ALS and Alzheimer's disease (32,35–37).

Our results demonstrate, for the first time, a genetic link between *Caz* and *ter94*, the *Drosophila* orthologs of *FUS* and *VCP*, respectively. Although it would be necessary to confirm whether that is *Drosophila*-specific or not, our results suggest genetic interaction between *FUS* and *VCP* in human. Genetic interaction between TDP-43 and VCP in *Drosophila* was demonstrated previously; IBMPFD-causing mutations in *ter94* lead to redistribution of TDP-43, from the nucleus to the cytoplasm, and redistribution of TDP-43 is sufficient to induce morphologically aberrant rough eyes (24). This previous report suggests that VCP can balance the amount of TDP-43, which is a constituent of larger heteronuclear ribonucleoprotein (hnRNP) complexes, between nucleus and cytoplasm by acting as a nucleocytoplasmic shuttling molecule (Fig. 6). In this schema, VCP functions to remove TDP-43 from RNP complexes, import TDP-43 into nuclei and degrade TDP-43 via autophagy (24,38,39). VCP might have similar functions with respect to FUS because FUS and TDP-43 have significant structural and functional similarities and are implicated in similar molecular processes (40–42). For example, TDP-43 and FUS act in the context of larger hnRNP complexes. FUS also continuously moves between the nucleus and the cytoplasm (16,17,43,44); therefore, FUS not only regulates gene expression in the nucleus, but also has important functions in the cytoplasm (5). Here, we showed that the decreased level of Caz in the nucleus and the resultant motor disturbance induced by neuron-specific *Caz*-knockdown could be rescued by overexpressed wild-type *ter94* despite lacking any change of Caz protein in the CNS (Supplementary Material, Fig. S1A and B). If VCP has a shuttling function as shown in Figure 6, wild-type ter94 overexpression could translocate Caz from cytoplasm to nucleus because nuclear importing function of ter94 would be dominantly induced in the situation with the deficiency of Caz in the nucleus. Conversely, the loss-of-function allele of *ter94* (*ter94*^{k15502}) exacerbated the depletion of *Caz* from the nucleus probably because ter94-mediated nuclear import of Caz was compromised.

It has been demonstrated that a polyQ tract can interact with VCP in *Drosophila* (34); specifically, either the strongest (*ter94*^{k15502}) or strong (*ter94*^{03775}) loss-of-function allele of *ter94* suppressed the eye degeneration induced by an expanded polyQ tract, whereas the overexpression of wild-type *ter94* in the background of *Caz*-knockdown enhanced this phenotype. Additionally, a chromosomal deletion of 46C3–46E02, the genomic region that contains *ter94*, acted as a dominant suppressor of the polyQ-induced phenotype (34). Our present study and these previous reports together indicate that gain and loss of *ter94* function rescued and exacerbated *Caz*-knockdown phenotypes, respectively, and that they had the converse effects on polyQ-induced phenotypes. These converse effects could be explained by the difference in disease pathogenesis; in polyQ-induced disease models, polyQ-containing pathogenic aggregates exist in nuclei of affected neurons; in contrast, Caz expression in nuclei is deficient in *Caz*-knockdown disease models. Overexpression of wild-type *ter94*, which functions in nuclear import of polyQ or Caz, would exacerbate nuclear polyQ aggregation, but could alleviate the nuclear deficiency of Caz protein.

Neuron-specific *Caz*-knockdown flies showed an age-dependent decline in climbing ability that was significantly worse than driver control flies for every age examined after day 7. Overexpression of wild-type *ter94* significantly rescued the declined locomotor ability caused by *Caz*-knockdown up to day 14, but it did not rescue the phenotype at later stages. Regarding the age-dependent ability to rescue locomotive deficits, we considered the two following possible explanations. First, the elongation of the branch length of MN terminals at NMJs caused by overexpression of wild-type *ter94* in neuron-specific *Caz*-knockdown flies may have alleviated the locomotive defects caused by neuron-specific *Caz*-knockdown. However, the extent of this elongation was highly variable. A previous report showed that larvae with NMJ overgrowth phenotypes exhibited mobility defects; this finding indicates that the elongation of nerve terminal branches beyond some adequate

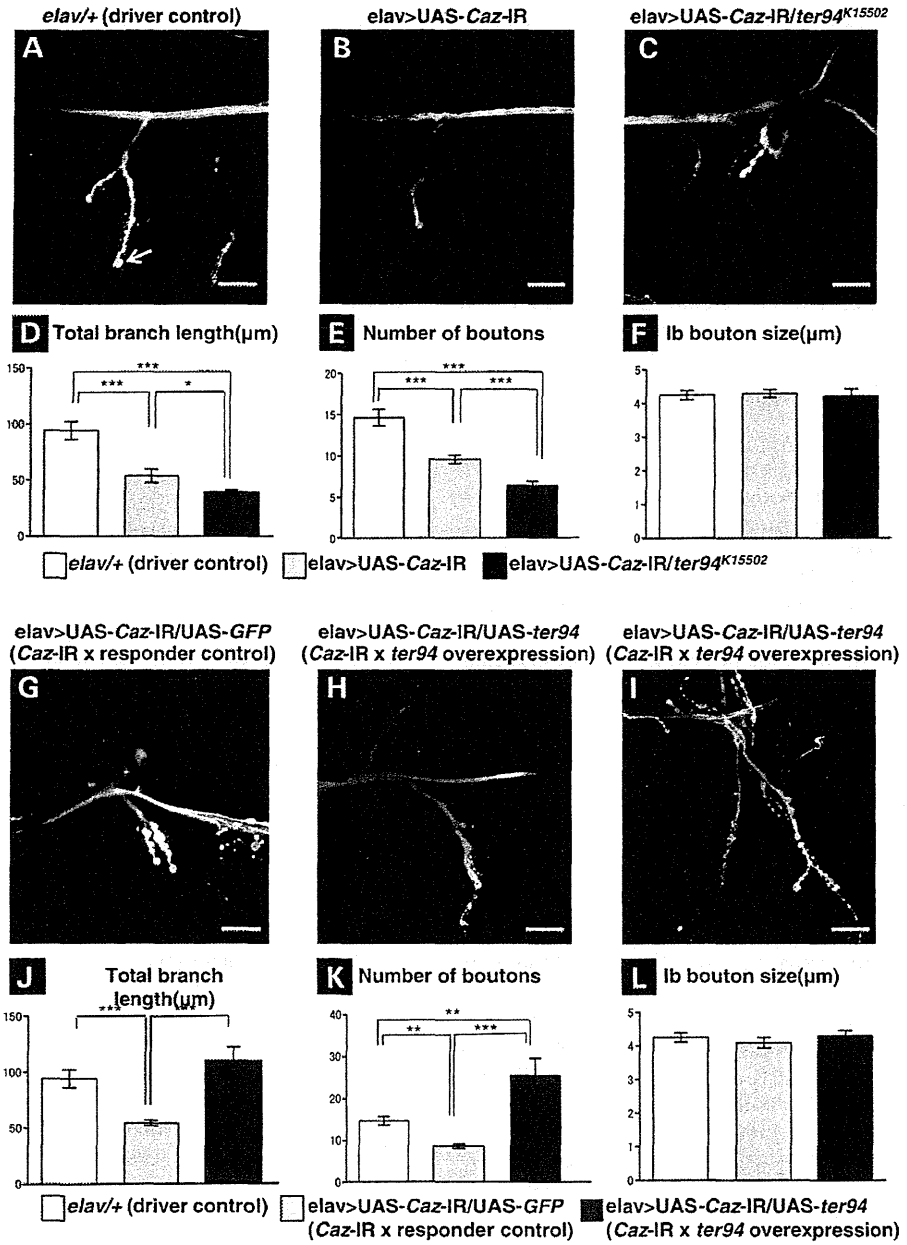

Figure 5. A loss-of-function *ter94* mutation and wild-type *ter94* overexpression change the morphology of MN presynaptic terminals in the NMJ of MN4 in neuron-specific *Caz*-knockdown larvae in opposite ways. A representative image of anti-horseradish peroxidase staining of muscle 4 synapses in third instar larvae with *elav/+* (**A**; a driver control), neuron-specific *Caz*-knockdown (**B**; elav>UAS-*Caz*-IR), neuron-specific *Caz*-knockdown crossed with the strongest loss-of-function mutation of *ter94* (**C**; elav>UAS-*Caz*-IR/*ter94*^{K15502}), neuron-specific *Caz*-knockdown crossed with UAS-*GFP* (**G**; elav>UAS-*Caz*-IR/UAS-*GFP*; a responder control) or neuron-specific *Caz*-knockdown crossed with UAS-*ter94* (**H** and **I**; different larvae with the same genotype, elav>UAS-*Caz*-IR/UAS-*ter94*). (**D** and **J**) Total branch length of the NMJ from muscle 4 for each of the indicated genotypes. Compared with the total length of synaptic branches of MNs in driver control larvae (A), that in neuron-specific *Caz*-knockdown larvae (B) is significantly decreased ($P < 0.001$, $n = 10$, D). This decrease in branch length observed in the neuron-specific *Caz*-knockdown larvae (B) is significantly worsened in larvae carrying the strongest loss-of-function allele of *ter94* and neuron-specific *Caz*-knockdown (C) ($P < 0.05$, $n = 10$, D). Conversely, the total branch length in larvae that overexpressed wild-type *ter94* in the background of neuron-specific *Caz*-knockdown (H and I) is significantly longer than that in larvae carrying elav>UAS-*Caz*-IR/UAS-*GFP* (G) ($P < 0.001$, $n = 14$, J). The extent of increase in the total branch length of elav>UAS-*Caz*-IR/UAS-*ter94* was highly variable among individual flies (H and I). The total branch length of synaptic branches of MNs in the larvae carrying elav>UAS-*Caz*-IR/UAS-*GFP* is significantly decreased compared with that of larvae carrying *elav/+* ($P < 0.001$, $n = 12$, J). (**E** and **K**) The number of synaptic boutons for each of the indicated genotypes. The number of synaptic boutons of MNs in neuron-specific *Caz*-knockdown larvae (B) is also significantly decreased compared with driver control larvae (A) ($P < 0.001$, $n = 10$, E). This decrease in the number of synaptic boutons in the neuron-specific *Caz*-knockdown larvae is significantly worsened in larvae carrying the strongest loss-of-function allele of *ter94* and neuron-specific *Caz*-knockdown (C) ($P < 0.001$, $n = 10$, E). Conversely, the number of synaptic boutons in the larvae carrying wild-type *ter94* overexpression in the background of neuron-specific *Caz*-knockdown (H and I) is significantly higher than that in responder control larvae (G) ($P < 0.001$, $n = 10$, K). Compared with the larvae carrying *elav/+*, the number of synaptic

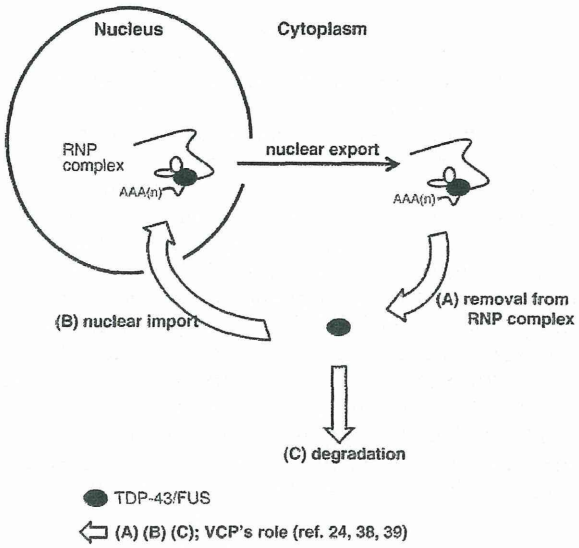

Figure 6. Hypothetical roles of VCP in the nucleoplasmic balance of TDP-43 and FUS referring to the paper by Ritson *et al.* (24). VCP, human ortholog of ter94, may act during removal of TDP-43/FUS from RNP complexes in the cytoplasm (**A**), nuclear import of TDP-43/FUS (**B**) and degradation of TDP-43/FUS by the autophagic pathway (**C**). FUS, the human ortholog of Caz, might translocate from cytoplasm to nucleus when VCP is overexpressed because the nuclear-import function of VCP (B) would be dominantly induced under conditions of FUS deficiency in nuclei. Conversely, loss-of-function alleles of VCP may exacerbate the FUS deficiency in nuclei because FUS is not being properly imported into nuclei by VCP.

length could cause disturbances in locomotive ability (45). Therefore, synaptic MN terminals may have to be within some optimal range of lengths. Second, the age-dependence of ability to rescue the locomotive defects might be due to the age-dependent difference in the expression levels of ter94. Tissue expression data from FlyBase (http://flybase.org) show that mRNA expression levels of *ter94* are very high in the CNS of third instar larvae, but they are relatively low in the head, eye or brain of adults. Age-dependent changes in ter94 expression levels might determine the period within which wild-type ter94 overexpression can rescue locomotive deficits caused by *Caz*-knockdown. Age-dependent effects of ter94 are also evident in fly models of polyQ-induced neurodegeneration. Between the third instar larval stage and the late pupal stage, levels of ter94 were elevated, and elevated levels of ter94 induced severe apoptotic cell death in those pupae (34).

In some IBMPFD-associated VCP mutants, it was previously reported that pathogenic VCPs could bind to cofactors, such as Npl4, Ufd1 or p47, more efficiently than wild-type VCP (46,47). However, little is known about which of the VCP cofactors relate to FUS-nuclear translocation or how the conformational change of VCP affects the interactions of VCP cofactors with other proteins.

In conclusion, we found a genetic interaction between *Caz* and *ter94*. Our data indicate that chemicals that up-regulate the function of VCP or facilitate nuclear import of FUS may suppress the pathogenic processes that lead to the degeneration of MNs in FUS-associated ALS/FTLD. This might be the first step to develop candidate drugs for the disease-modifying therapy of human ALS.

MATERIALS AND METHODS

Fly stocks

Fly stocks were maintained at 25°C on standard food containing 0.7% agar, 5% glucose and 7% dry yeast. Canton S was used as the wild-type strain. The strain: w^{1118}; *P {w [+mC] = UAS-GFP. nls} 14* (DGRC number 107870) (UAS-*GFP*) and chromosomal deficiency line: *Df (2R) X1*, $Mef2^{X1}$/*CyO*, Adh^{nB} (DGRC number 106718) were obtained from the Kyoto *Drosophila* Genetic Resource Center. The strains: *w* [*]; *P {[+mC] = GAL4-elav.L} 3* (Bloomington BL8760) (*elav-GAL4*), $y^1 w$ [*]; *P {[+mC] = Act5C-GAL4} 17bFO1/TM6B*, Tb^1 (BL3954) (*Act5C-GAL4*), $y^1 w^{67c23}$; *P {w [+mC] = lacW} ter94*^{K15502}/*CyO* (BL10454) (*ter94*^{K15502}) and $cn^1 P$ {*ry* [+*t7.2*] = *PZ*} *ter94*^{03775}/*CyO*; ry^{506} (BL11349) (*ter94*^{03775}) were obtained from the Bloomington *Drosophila* stock center in Indiana. Establishment of the lines carrying *GMR-GAL4* was as described previously (48). We crossed transgenic UAS-*Caz*-IR flies with *Act5C-GAL4*, *GMR-GAL4* or *elav-GAL4* flies to drive expression of *Caz* dsRNA throughout the whole body of flies, specifically in eye imaginal discs or specifically in neuronal tissues, respectively. We generated eye-specific *Caz*-knockdown flies (*GMR-GAL4*; UAS-*Caz*-IR/+; +) (GMR>UAS-*Caz*-IR) and neuron-specific Caz-knockdown flies (w; UAS-*Caz*-IR/+; *elav-GAL4*/+) (elav>UAS-*Caz*-IR). Each transgenic strain showed a consistent phenotype (Table 1).

Dr Kakizuka kindly provided UAS-*ter94* flies. The UAS-*ter94*-IR strain: w^{1118}; *P {GD9777} v24354* (VDRC number v24354) (*ter94*-knockdown) was obtained from the VDRC. VDRC reports that the *ter94*-RNAi construct is inserted into chromosome 2 and has no off-target effects. The lines generated in this study are as follows: *GMR-GAL4*; +; + (*GMR*), *GMR-GAL4*; UAS-*Caz*-IR363−399/+; + (GMR>UAS-*Caz*-IR), *GMR-GAL4*; UAS-*Caz*-IR363−399/UAS-*Caz*-IR363−399; + (GMR>UAS-*Caz*-IR/UAS-*Caz*-IR), *GMR-GAL4*; UAS-*Caz*-IR363−399/*ter94*^{K15502}; + (GMR>UAS-*Caz*-IR/*ter94*^{K15502}), *GMR-GAL4*; UAS-*Caz*-IR363−399/*ter94*^{03775}; + (GMR>UAS-*Caz*-IR/*ter94*^{03775}), *GMR-GAL4*; UAS-*Caz*-IR363−399/UAS-*GFP*; + (GMR>UAS-*Caz*-IR/UAS-*GFP*), *GMR-GAL4*; UAS-*Caz*-IR363−399/UAS-*ter94*; + (GMR>UAS-*Caz*-IR/UAS-*ter94*), w; +; *elav-GAL4*/+ (*elav*/+; a driver control), UAS-*Caz*-IR363−399/+ (UAS-*Caz*-IR/+; a responder control), *ter94*^{K15502}/+, w; UAS-*Caz*-IR363−399/+; *elav-GAL4*/+ (elav> UAS-*Caz*-IR), w; UAS-*Caz*-IR363−399/UAS-*Caz*-IR363−399;

boutons is significantly decreased in the larvae carrying elav>UAS-*Caz*-IR/UAS-*GFP* ($P < 0.001$, $n = 10$, K), but significantly increased in those carrying elav> UAS-*Caz*-IR/UAS-*ter94* ($P < 0.05$, $n = 14$, K). (**F** and **L**) The size of synaptic boutons for each of the indicated genotypes. The size of Ib bouton (indicated with an arrow in A) was measured ($n = 31$ for *elav*/+, $n = 33$ for elav>UAS-*Caz*-IR, $n = 31$ for elav>UAS-*Caz*-IR/*ter94*^{K15502}, $n = 30$ for elav>UAS-*Caz*-IR/UAS-*GFP* and $n = 32$ for elav>UAS-*Caz*-IR/UAS-*ter94*). There are no significant differences in the size of synaptic boutons among driver control larvae, either larvae with elav>UAS-*Caz*-IR and those with elav>UAS-*Caz*-IR/*ter94*^{K15502} (F) or among driver control larvae, either larvae with elav>UAS-*Caz*-IR/UAS-*GFP* and elav>

elav-GAL4/elav-GAL4 (elav>UAS-*Caz*-IR/UAS-*Caz*-IR), w; UAS-*Caz*-IR363–399/*ter94*^{K15502}; *elav-GAL4/+* (elav>UAS-*Caz*-IR/*ter94*^{K15502}), w; UAS-*Caz*-IR363–399/UAS-*GFP*; *elav-GAL4/+* (elav>UAS-*Caz*-IR/UAS-*GFP*), w; UAS-*Caz*-IR363–399/UAS-*ter94*; *elav-GAL4/+* (elav>UAS-*Caz*-IR/UAS-*ter94*).

Immunohistochemistry

Rabbit anti-Caz antibodies were raised against amino acid residues 29–45 and 383–399 of Caz and were produced previously (19). For immunohistochemical analysis, CNS tissues were dissected from third instar larvae and fixed in 4% paraformaldehyde/phosphate buffered saline (PBS) for 15 min at 25°C. These tissue samples were washed with PBS containing 0.3% Triton X-100; fixed samples were then incubated with Alexa 488-conjugated phalloidin (1 unit/200 μl) in PBS containing 0.3% Triton X-100 for 20 min at 25°C. The samples were then blocked with blocking buffer (PBS containing 0.15% Triton X-100 and 10% normal goat serum) for 30 min at 25°C, and then incubated with 1 : 1000 diluted rabbit anti-Caz antibody in the blocking buffer for 20 h at 4°C. After extensive washing with PBS containing 0.3% Triton X-100, samples were incubated in the dark with secondary antibodies labeled with Alexa 546 (1 : 400; Invitrogen) diluted in the blocking buffer for 3 h at 25°C. After washing with PBS containing 0.3% Triton X-100, the samples were stained with DAPI (0.5 μg/ml)/PBS/0.1% Triton X-100. After extensive washing with PBS containing 0.1% Triton X-100 and PBS, the samples were mounted in Vectashield (Vector Laboratories-Inc.) and observed under a confocal laser scanning microscope (OLYMPUS FLUOVIEW FV10i). Images were analyzed with the program MetaMorph Imaging System 7.7 (Molecular Devices Inc.). The use of this program made it possible to quantify the average and the standard error of fluorescence emission from nuclei of each fly strain.

For NMJ staining, third instar larvae were dissected in HL3 saline (49), and then fixed in 4% paraformaldehyde/PBS for 30 min. The blocking buffer contained 2% bovine serum albumin and 0.1% Triton X-100 in PBS. Fluorescein isothiocyanate-conjugated goat anti-horseradish peroxidase (HRP) (1:1000, MP Biochemicals) was used as the detection antibody. The samples were mounted and observed under a confocal laser scanning microscope (Carl Zeiss LSM510, Jena, Germany). MN 4 (Ib) in muscle 4 in abdominal segment 2 was quantified. Images were acquired using a Zeiss LSM 510 confocal laser scanning microscope by merging 1 μm interval z-sections onto a single plane. The MetaMorph imaging system was used to measure nerve terminal branch lengths and Ib bouton sizes.

Immunoblotting analysis

Protein extracts from the CNS of *Drosophila* carrying *elav/+*, elav>UAS-*Caz*-IR, elav>UAS-*Caz*-IR/*ter94* ^{K15502}, elav>UAS-*Caz*-IR/UAS-*GFP* and elav>UAS-*Caz*-IR/UAS-*ter94* larvae were prepared as described previously (19). Briefly, the CNS was excised from third instar larvae and homogenized in a sample buffer containing 50 mM Tris–HCl (pH 6.8), 2% sodium dodecyl sulfate (SDS), 10% glycerol, 0.1% bromophenol blue and 1.2% β-mercaptoethanol. The homogenates were boiled at 100°C for 5 min and then centrifuged. The supernatants (extracts) were electrophoretically separated on SDS-polyacrylamide gels containing 12% acrylamide and then transferred to polyvinylidene difluoride membranes (Merck, Millipore, MA, USA). The blotted membranes were blocked with tris-buffered saline/0.05% Tween containing 5% skim milk for 1 h at 25°C, followed by incubation with rabbit polyclonal anti-Caz at a 1:5000 dilution for 16 h at 4°C. After washing, the membranes were incubated with HRP-conjugated anti-rabbit IgG (Thermo Scientific, IL, USA) at 1:10 000 dilution for 2 h at 25°C. Antibody binding was detected using ECL Western blotting detection reagents (Thermo Scientific) and images were analyzed using an ImageQuant^{TM} LAS 4000 image analyzer (GE Healthcare Bioscience, Tokyo, Japan). To compare Caz protein levels in the CNS extracts of those larvae, densitometric quantification of the 45-kDa Caz protein bands was carried out. The relative band intensities were quantified and normalized to Coomassie Brilliant Blue staining, then expressed as the percentage of the band intensity derived from larvae carrying *elav/+*.

Scanning electron microscopy

Adult flies were anesthetized with 99% diethyl ether, mounted on stages and observed under an SEM V-7800 (Keyence Inc.) in the low vacuum mode (50). In every experiment, at least five adult flies were chosen from each line for scanning electron microscopy to assess the eye phenotype. For each experiment, there was no significant variation in eye phenotype among the five individuals from the same strain.

Longevity assay

Longevity assays were carried out in a humidified, temperature-controlled incubator set at 25°C and 60% humidity on a 12-h light and 12-h dark cycle; flies were maintained on standard fly food. Flies carrying *elav/+* ($n = 151$), elav>UAS-*Caz*-IR ($n = 123$), elav>UAS-*Caz*-IR/*ter94*^{K15502} ($n = 120$), elav>UAS-*Caz*-IR/UAS-*GFP* ($n = 140$) or elav>UAS-*Caz*-IR/UAS-*ter94* ($n = 140$) were placed at 28°C, and newly eclosed adult male flies were separated and placed in vials at a low density (20 flies per vial). Every 3 days, they were transferred to new tubes containing fresh food and deaths were scored. The survival rate was determined by plotting a graph of the percentage of surviving flies among total flies at the starting point of each experiment versus days.

Climbing assay

Climbing assays were performed as described previously (29). Flies carrying *elav/+*, UAS-*Caz*-IR/+, *ter94*^{K15502}/+, elav>UAS-*Caz*-IR, elav>UAS-*Caz*-IR/*ter94*^{K15502}, elav>UAS-*Caz*-IR/UAS-*GFP* and elav>UAS-*Caz*-IR/UAS-*ter94* were placed at 28°C, and newly eclosed adult male flies were separated and placed in vials at a density of 20 flies per vial. Flies were transferred, without anesthesia, to a conical tube. The tubes were tapped to collect the flies to the bottom, and they were then given 30 s to climb the wall. After 30 s, the flies were collected at the bottom by tapping of the tube and were again allowed to climb for 30 s. Similar procedures, all of which were videotaped, were repeated five times in total. For each climbing experiment, the height to which each fly

climbed was scored as score (height climbed); 0 (less than 2 cm), 1 (between 2 and 3.9 cm), 2 (between 4 and 5.9 cm), 3 (between 6 and 7.9 cm), 4 (between 8 and 9.9 cm) or 5 (greater than 10 cm). The climbing index for each fly strain was calculated as follows; each score was multiplied by the number of flies for which that score was recorded, and the products were summed up, then divided by five times the total number of flies examined. These climbing assays were carried out every 7 days until the 28th day after eclosion.

Data analysis

GraphPad Prism version 6.0 was used to perform each statistical analysis. The Mann–Whiney test was used for the assessment of the statistical significance of comparisons between two groups of data. For other assays, one-way analysis of variance (ANOVA) was used to determine the statistical significance of comparisons between groups of data. When the two-way ANOVA showed significant variation among groups, a subsequent Dunnett's test was used for pairwise comparisons between groups. All data are shown as mean ± standard error (SE).

SUPPLEMENTARY MATERIAL

Supplementary Material is available at *HMG* online.

ACKNOWLEDGEMENTS

We would like to thank Dr Kakizuka for generously providing us the UAS-*ter94* fly strains used in these experiments. We would also like to acknowledge Dr H. Yoshida, Ms R. Sahashi, Mr K. Morishita and Mr K. Shimaji for valuable discussion, technical support and suggestions. We thank the Bloomington *Drosophila* stock center, the Vienna *Drosophila* RNAi center and Kyoto *Drosophila* Genetic Resource Center for giving us fly lines.

Conflict of Interest statement. None declared.

FUNDING

This work was supported by Grants-in-Aid from the Research Committee of CNS. Degenerative Diseases, the Ministry of Health, Labour and Welfare of Japan (T.T.), and partly supported by "Integrated Research on Neuropsychiatric Disorders" carried out under the Strategic Research Program for Brain Sciences by the Ministry of Education, Culture, Sports, Science and Technology of Japan (Y.N.). The funders had no role in study design, data collection and analysis, decision to publish or preparation of the manuscript.

REFERENCES

1. Boillée, S., Vande Velde, C. and Cleveland, D.W. (2006) ALS: a disease of motor neurons and their nonneuronal neighbors. *Neuron*, **52**, 39–59.
2. Mackenzie, I.R., Rademakers, R. and Neumann, M. (2010) TDP-43 and FUS in amyotrophic lateral sclerosis and frontotemporal dementia. *Lancet Neurol.*, **9**, 995–1007.
3. Lomen-Hoerth, C., Anderson, T. and Miller, B. (2002) The overlap of amyotrophic lateral sclerosis and frontotemporal dementia. *Neurology*, **59**, 1077–1079.
4. Murphy, J.M., Henry, R.G., Langmore, S., Kramer, J.H., Miller, B.L. and Lomen-Hoerth, C. (2007) Continuum of frontal lobe impairment in amyotrophic lateral sclerosis. *Arch. Neurol.*, **64**, 530–534.
5. Dormann, D. and Haass, C. (2013) Fused in sarcoma (FUS): an oncogene goes awry in neurodegeneration. *Mol. Cell Neurosci.*, **56**, 475–486.
6. Lemmens, R., Moore, M.J., Al-Chalabi, A., Brown, R.H. Jr. and Robberecht, W. (2010) RNA metabolism and the pathogenesis of motor neuron diseases. *Trends Neurosci.*, **33**, 249–258.
7. Gitcho, M.A., Baloh, R.H., Chakraverty, S., Mayo, K., Norton, J.B., Levitch, D., Hatanpaa, K.J., White, C.L. 3rd., Bigio, E.H., Caselli, R. *et al.* (2008) TDP-43 A315 T mutation in familial motor neuron disease. *Ann. Neurol.*, **63**, 535–538.
8. Yokoseki, A., Shiga, A., Tan, C.F., Tagawa, A., Kaneko, H., Koyama, A., Eguchi, H., Tsujino, A., Ikeuchi, T., Kakita, A. *et al.* (2008) TDP-43 mutation in familial amyotrophic lateral sclerosis. *Ann. Neurol.*, **63**, 538–542.
9. Kabashi, E., Valdmanis, P.N., Dion, P., Spiegelman, D., McConkey, B.J., Vande Velde, C., Bouchard, J.P., Lacomblez, L., Pochigaeva, K., Salachas, F. *et al.* (2008) TARDBP mutations in individuals with sporadic and familial amyotrophic lateral sclerosis. *Nat. Genet.*, **40**, 572–574.
10. Sreedharan, J., Blair, I.P., Tripathi, V.B., Hu, X., Vance, C., Rogelj, B., Ackerley, S., Durnall, J.C., Williams, K.L., Buratti, E. *et al.* (2008) TDP-43 mutations in familial and sporadic amyotrophic lateral sclerosis. *Science*, **319**, 1668–1672.
11. Pesiridis, G.S., Lee, V.M. and Trojanowski, J.Q. (2009) Mutations in TDP-43 link glycine-rich domain functions to amyotrophic lateral sclerosis. *Hum. Mol. Genet.*, **18**, R156–R162.
12. Kwiatkowski, T.J. Jr., Bosco, D.A., Leclerc, A.L., Tamrazian, E., Vanderburg, C.R., Russ, C., Davis, A., Gilchrist, J., Kasarskis, E.J., Munsat, T. *et al.* (2009) Mutations in the FUS/TLS gene on chromosome 16 cause familial amyotrophic lateral sclerosis. *Science*, **323**, 1205–1208.
13. Vance, C., Rogelj, B., Hortobágyi, T., De, Vos, K.J., Nishimura, A.L., Sreedharan, J., Hu, X., Smith, B., Ruddy, D., Wright, P. *et al.* (2009) Mutations in FUS, an RNA processing protein, cause familial amyotrophic lateral sclerosis type 6. *Science*, **323**, 1208–1211.
14. Hewitt, C., Kirby, J., Highley, J.R., Hartley, J.A., Hibberd, R., Hollinger, H.C., Williams, T.L., Ince, P.G., McDermott, C.J. and Shaw, P.J. (2010) Novel FUS/TLS mutations and pathology in familial and sporadic amyotrophic lateral sclerosis. *Arch. Neurol.*, **67**, 455–461.
15. Rademakers, R., Stewart, H., Dejesus-Hernandez, M., Krieger, C., Graff-Radford, N., Fabros, M., Briemberg, H., Cashman, N., Eisen, A. and Mackenzie, I.R. (2010) Fus gene mutations in familial and sporadic amyotrophic lateral sclerosis. *Muscle Nerve*, **42**, 170–176.
16. Zinszner, H., Sok, J., Immanuel, D., Yin, Y. and Ron, D. (1997) TLS (FUS) binds RNA in vivo and engages in nucleo-cytoplasmic shuttling. *J. Cell Sci.*, **110**, 1741–1750.
17. Lagier-Tourenne, C., Polymenidou, M. and Cleveland, D.W. (2010) TDP-43 and FUS/TLS: emerging roles in RNA processing and neurodegeneration. *Hum. Mol. Genet.*, **19**, R46–R64.
18. Feiguin, F., Godena, V.K., Romano, G., D'Ambrogio, A., Klima, R. and Baralle, F.E. (2009) Depletion of TDP-43 affects *Drosophila* motoneurons terminal synapsis and locomotive behavior. *FEBS Lett.*, **583**, 1586–1592.
19. Sasayama, H., Shimamura, M., Tokuda, T., Azuma, Y., Yoshida, T., Mizuno, T., Nakagawa, M., Fujikake, N., Nagai, Y. and Yamaguchi, M. (2012) Knockdown of the *Drosophila* fused in sarcoma (FUS) homologue causes deficient locomotive behavior and shortening of motoneuron terminal branches. *PLoS One*, **7**, e39483.
20. Kabashi, E., Bercier, V., Lissouba, A., Liao, M., Brustein, E., Rouleau, G.A. and Drapeau, P. (2011) FUS and TARDBP but not SOD1 interact in genetic models of amyotrophic lateral sclerosis. *PLoS Genet.*, **7**, e1002214.
21. Wang, J.W., Brent, J.R., Tomlinson, A., Shneider, N.A. and McCabe, B.D. (2011) The ALS-associated proteins FUS and TDP-43 function together to affect *Drosophila* locomotion and life span. *J. Clin. Invest.*, **121**, 4118–4126.
22. Meyer, H., Bug, M. and Bremer, S. (2012) Emerging functions of the VCP/p97 AAA-ATPase in the ubiquitin system. *Nat. Cell Biol.*, **14**, 117–123.
23. Braun, R.J. and Zischka, H. (2008) Mechanisms of Cdc48/VCP-mediated cell death: from yeast apoptosis to human disease. *Biochim. Biophys. Acta*, **1783**, 1418–1435.

24. Ritson, G.P., Custer, S.K., Freibaum, B.D., Guinto, J.B., Geffel, D., Moore, J., Tang, W., Winton, M.J., Neumann, M., Trojanowski, J.Q. *et al.* (2010) TDP-43 mediates degeneration in a novel *Drosophila* model of disease caused by mutations in VCP/p97. *J. Neurosci.*, **30**, 7729–7739.
25. Watts, G.D., Wymer, J., Kovach, M.J., Mehta, S.G., Mumm, S., Darvish, D., Pestronk, A., Whyte, M.P. and Kimonis, V.E. (2004) Inclusion body myopathy associated with Paget disease of bone and frontotemporal dementia is caused by mutant valosin-containing protein. *Nat. Genet.*, **36**, 377–381.
26. Johnson, J.O., Mandrioli, J., Benatar, M., Abramzon, Y., Van, Deerlin, V.M., Trojanowski, J.Q., Gibbs, J.R., Brunetti, M., Gronka, S., Wuu, J. *et al.* (2010) Exome sequencing reveals VCP mutations as a cause of familial ALS. *Neuron*, **68**, 857–864.
27. Stolow, D.T. and Haynes, S.R. (1995) Cabeza, a *Drosophila* gene encoding a novel RNA binding protein, shares homology with EWS and TLS, two genes involved in human sarcoma formation. *Nucleic Acids Res.*, **23**, 835–843.
28. Ruden, D.M., Sollars, V., Wang, X., Mori, D., Alterman, M. and Lu, X. (2000) Membrane fusion proteins are required for oskar mRNA localization in the *Drosophila* egg chamber. *Dev. Biol.*, **218**, 314–325.
29. Shcherbata, H.R., Yatsenko, A.S., Patterson, L., Sood, V.D., Nudel, U., Yaffe, D., Baker, D. and Ruohola-Baker, H. (2007) Dissecting muscle and neuronal disorders in a *Drosophila* model of muscular dystrophy. *EMBO J.*, **26**, 481–493.
30. Chang, H.C., Dimlich, D.N., Yokokura, T., Mukherjee, A., Kankel, M.W., Sen, A., Sridhar, V., Fulga, T.A., Hart, A.C., Van Vactor, D. *et al.* (2008) Modeling spinal muscular atrophy in *Drosophila*. *PLoS One*, **3**, e3209.
31. Chee, F., Mudher, A., Newman, T.A., Cuttle, M., Lovestone, S. and Shepherd, D. (2006) Overexpression of tau results in defective synaptic transmission in *Drosophila* neuromuscular junctions. Biochem. Soc. Trans., **34**, 88–90.
32. Hirabayashi, M., Inoue, K., Tanaka, K., Nakadate, K., Ohsawa, Y., Kamei, Y., Popiel, A.H., Sinohara, A., Iwamatsu, A., Kimura, Y. *et al.* (2001) VCP/p97 in abnormal protein aggregates, cytoplasmic vacuoles, and cell death, phenotypes relevant to neurodegeneration. *Cell Death Differ.*, **8**, 977–984.
33. Fujita, K., Nakamura, Y., Oka, T., Ito, H., Tamura, T., Tagawa, K., Sasabe, T., Katsuta, A., Motoki, K., Shiwaku, H. *et al.* (2013) A functional deficiency of TERA/VCP/p97 contributes to impaired DNA repair in multiple polyglutamine diseases. *Nat. Commun.*, **4**, 1816. doi:10.1038/ncomms2828.
34. Higashiyama, H., Hirose, F., Yamaguchi, M., Inoue, Y.H., Fujikake, N., Matsukage, A. and Kakizuka, A. (2002) Identification of ter94, *Drosophila* VCP, as a modulator of polyglutamine-induced neurodegeneration. *Cell Death Differ.*, **9**, 264–273.
35. Ishigaki, S., Hishikawa, N., Niwa, J., Iemura, S., Natsume, T., Hori, S., Kakizuka, A., Tanaka, K. and Sobue, G. (2004) Physical and functional interaction between Dorfin and Valosin-containing protein that are colocalized in ubiquitylated inclusions in neurodegenerative disorders. *J. Biol. Chem.*, **279**, 51376–51385.
36. Kakizuka, A. (2008) Roles of VCP in human neurodegenerative disorders. *Biochem. Soc. Trans.*, **36**, 105–108.
37. Mizuno, Y., Hori, S., Kakizuka, A. and Okamoto, K. (2003) Vacuole-creating protein in neurodegenerative diseases in humans. *Neurosci. Lett.*, **343**, 77–80.
38. Marti, F. and King, P.D. (2005) The p95–100 kDa ligand of the T cell-specific adaptor (TSAd) protein Src-homology-2 (SH2) domain implicated in TSAd nuclear import is p97 Valosin-containing protein (VCP). *Immunol. Lett.*, **97**, 235–243.
39. Ju, J.S. and Weihl, C.C. (2010) p97/VCP at the intersection of the autophagy and the ubiquitin proteasome system. *Autophagy*, **6**, 283–285.
40. Ling, S.C., Albuquerque, C.P., Han, J.S., Lagier-Tourenne, C., Tokunaga, S., Zhou, H. and Cleveland, D.W. (2010) ALS-associated mutations in TDP-43 increase its stability and promote TDP-43 complexes with FUS/TLS. *Proc. Natl Acad. Sci. USA*, **107**, 13318–13323.
41. van Blitterswijk, M. and Landers, J.E. (2010) RNA processing pathways in amyotrophic lateral sclerosis. *Neurogenetics*, **11**, 275–290.
42. Kim, S.H., Shanware, N.P., Bowler, M.J. and Tibbetts, R.S. (2010) Amyotrophic lateral sclerosis-associated proteins TDP-43 and FUS/TLS function in a common biochemical complex to co-regulate HDAC6 mRNA. *J. Biol. Chem.*, **285**, 34097–34105.
43. Fiesel, F.C. and Kahle, P.J. (2011) TDP-43 and FUS/TLS: cellular functions and implications for neurodegeneration. *FEBS J.*, **278**, 3550–3568.
44. Ayala, Y.M., Zago, P., D'Ambrogio, A., Xu, Y.F., Petrucelli, L., Buratti, E. and Baralle, F.E. (2008) Structural determinants of the cellular localization and shuttling of TDP-43. *J. Cell Sci.*, **121**, 3778–3785.
45. Nagai, R., Hashimoto, R. and Yamaguchi, M. (2010) *Drosophila* Syntrophins are involved in locomotion and regulation of synaptic morphology. *Exp. Cell Res.*, **316**, 2313–2321.
46. Fernández-Sáiz, V. and Buchberger, A. (2010) Imbalances in p97 co-factor interactions in human proteinopathy. *EMBO Rep.*, **11**, 479–485.
47. Manno, A., Noguchi, M., Fukushi, J., Motohashi, Y. and Kakizuka, A. (2010) Enhanced ATPase activities as a primary defect of mutant valosin-containing proteins that cause inclusion body myopathy associated with Paget disease of bone and frontotemporal dementia. *Genes Cells*, **15**, 911–922.
48. Takahashi, Y., Hirose, F., Matsukage, A. and Yamaguchi, M. (1999) Identification of three conserved regions in the DREF transcription factors from *Drosophila melanogaster* and *Drosophila virilis*. *Nucleic Acids Res.*, **27**, 510–516.
49. Stewart, B.A., Atwood, H.L., Renger, J.J., Wang, J. and Wu, C.F. (1994) Improved stability of *Drosophila* larval neuromuscular preparations in haemolymph-like physiological solutions. *J. Comp. Physiol. A*, **175**, 179–191.
50. Ly, L.L., Suyari, O., Yoshioka, Y., Tue, N.T., Yoshida, H. and Yamaguchi, M. (2013) dNF-YB plays dual roles in cell death and cell differentiation during *Drosophila* eye development. *Gene*, **520**, 106–118.

Supplementary Materials

Supplementary Figure 1. Immunoblotting analysis of the CNS extracts of third instar larvae. (A) A representative result of the analysis of protein extracts from the CNS of the *elav/+*, elav>UAS-*Caz*-IR, elav>UAS-*Caz*-IR/*ter94*^{K15502}, elav>UAS-*Caz*-IR/UAS-*GFP* and elav>UAS-*Caz*-IR/UAS-*ter94* larvae (n = 5, each). The blots are probed with the polyclonal anti-Caz antibody used in the previous study (19). A 45-kDa band (arrow) corresponds to the Caz protein. (B) Densitometric quantification of the 45-kDa bands in each fly strain used in (A). The intensity of the 45-kDa band which indicates the expression level of Caz protein is much weaker in larvae carrying elav>UAS-*Caz*-IR than in the larvae carrying *elav/+*. Besides, there is no apparent difference in the intensity of the Caz protein band between the larvae carrying elav>UAS-*Caz*-IR and elav>UAS-*Caz*-IR/*ter94*^{K15502}. Similarly, there is no apparent difference in the intensity of the band between the larvae carrying elav>UAS-*Caz*-IR/UAS-*GFP* and elav>UAS-*Caz*-IR/UAS-*ter94*.

Supplementary Figure 2. The locomotive ability of each control flies, which carry *elav/+* (a driver control, n = 255), UAS-*Caz*-IR/+ (a responder control, n = 250), *ter94*^{k15502}/+ (n = 235). There are no significant differences in climbing abilities among those fly lines in each day after eclosion that was monitored until 14 days.

Supplementary Figure 3. Life-span analyses of flies of each genotype. Percentage survival of adult male flies of the indicated genotype is shown. (A) There are no significant differences in life spans among the control flies carrying *elav/+* (n = 151), neuron-specific *Caz*-knockdown flies carrying elav>UAS-*Caz*-IR (n = 123), and flies

carrying elav>UAS-*Caz*-IR/*ter94*^{K15502} (n = 120). (B) Similarly, there are no significant differences in life spans between flies carrying elav>UAS-*Caz*-IR/UAS-*GFP* (n = 140) and those carrying elav>UAS-*Caz*-IR/UAS-*ter94* (n = 140).

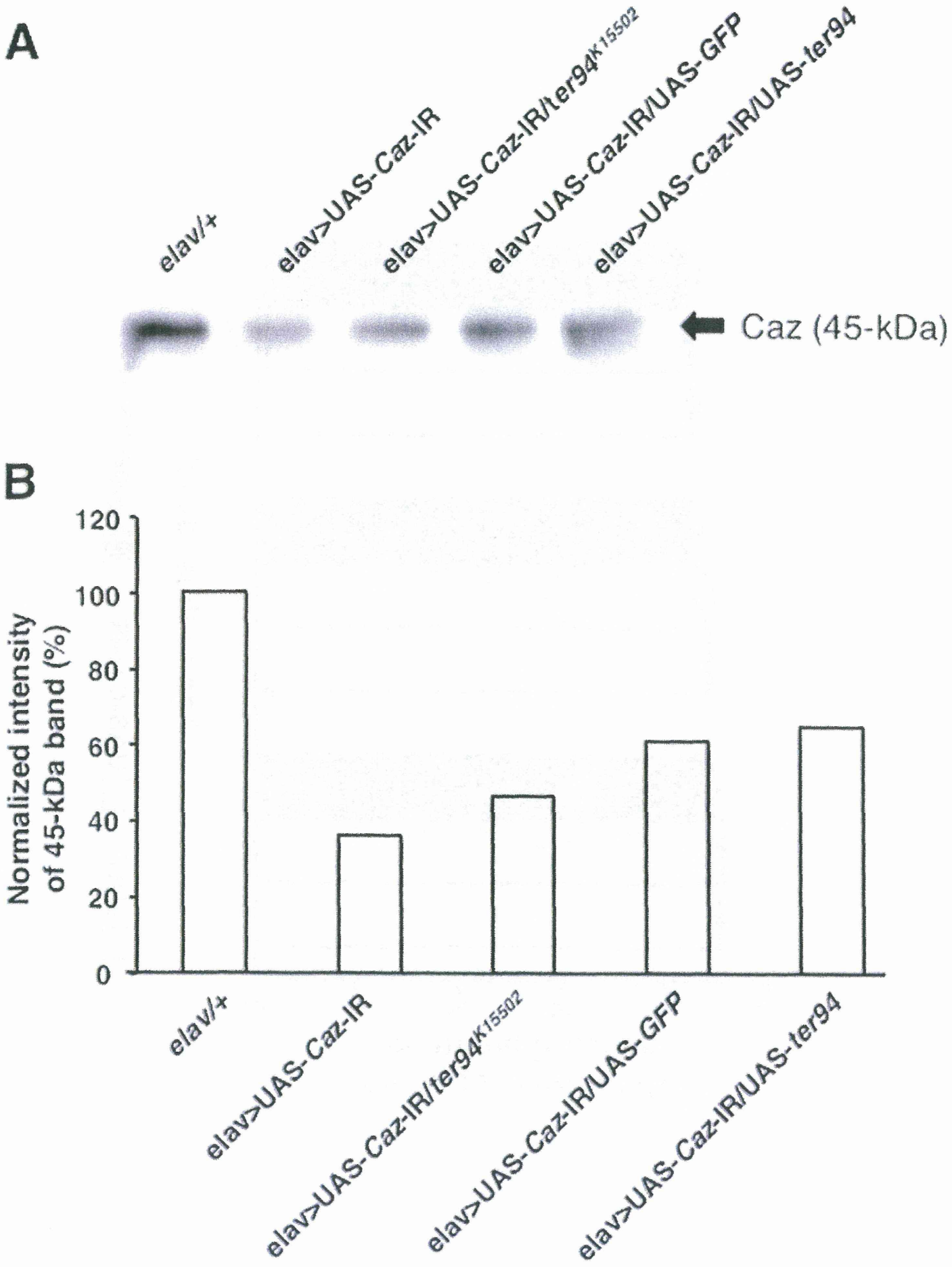
A
elav/+
elav>UAS-Caz-IR
elav>UAS-Caz-IR/ter94K15502
elav>UAS-Caz-IR/UAS-GFP
elav>UAS-Caz-IR/UAS-ter94
Caz (45-kDa)
B
Normalized intensity of 45-kDa band (%)
120
100
80
60
40
20
0
elav/+
elav>UAS-Caz-IR
elav>UAS-Caz-IR/ter94K15502
elav>UAS-Caz-IR/UAS-GFP
elav>UAS-Caz-IR/UAS-ter94